Longitudinal Breakdown Strength of Wet-mate Solid-Solid Interfaces at VLF and 50 Hz AC voltages

Erling Ildstad and Roger Dale
NTNU, Department of Electrical Power Engineering, Trondheim, Norway

Emre Kantar
SINTEF Energy Research, Department of Electrical Power Technology, Trondheim, Norway

Abstract

The 50 Hz AC breakdown strength of dry interfaces is known to strongly depend upon the mechanical properties, contact pressure, roughness of the surfaces, and the type of lubricant used at the interface.

This paper aims to experimentally examine how these factors affect the longitudinal AC breakdown strength of interfaces assembled in water, so-called wet interfaces. The main aim is to obtain data relevant to the design of power equipment operating at very low frequency (VLF) or DC voltages.

Experiments were conducted using identical specimens made from 4mm thick plaques of PMMA and plane sections cut from XLPE cable insulation. The findings were discussed with respect to expected dimensions of interface voids and contact regions, considering tribology-based contact theory, including the impact of surface roughness, modulus of elasticity, and applied mechanical interface pressure.

The longitudinal 50 Hz AC breakdown strength values of wet samples were typically as low as 80 % of samples assembled in the air under dry conditions. In addition, the results verified previous findings that the AC breakdown strength strongly increases with reduced surface roughness, stiffness, and increased interface pressure.

The breakdown values obtained during VLF breakdown testing were found to be 2 – 3 times higher than in the case of testing at 50 Hz AC voltages.

1. Introduction

Tangentially energized interfaces constitute critical parts of many important insulation systems, such as power cable joints and terminations, outdoor composite insulators, and subsea wet-mate and break connectors and penetrators. Due to variable degree of surface smoothness or surface roughness, small voids and contact areas are formed along the interface, a phenomenon schematically illustrated in Fig. 1.

Several previous studies have shown a significant increase in longitudinal AC 50 Hz breakdown strength by increasing the interface contact pressure, reducing the surface roughness, filling the surface voids with insulating lubricant, and applying softer, rubber-type materials [1]–[14].

During this work, the validity of some of these findings was re-examined. The main aim has, however, been to obtain relevant data useful for the design of power equipment operating at very low frequency (VLF) or DC voltages. Most experiments were performed using samples assembled in tap water, so-called wet-mate samples. This was done to limit the scope, simplify interpretation, and facilitate the application of the results in the development of design criteria for outdoor and subsea power accessories.

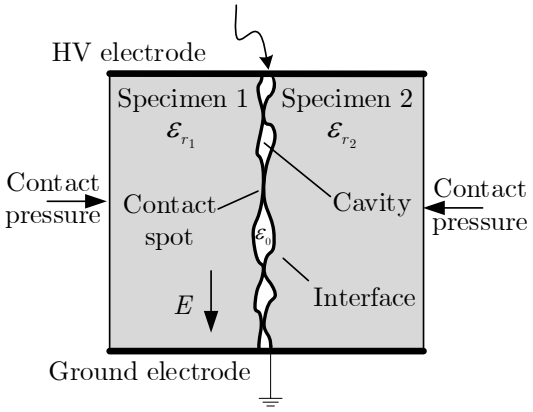

Fig. 1 – Schematic illustration of a solid-solid interface with voids and contact regions caused by surface roughness (imperfect surfaces). Reprinted, with permission, from [12].

2. Theoretical background

One of the earliest models describing the interface of contact between two solids is the so-called GW model, named after Greenwood and Williamson [15]. This tribological or friction model considers the interface as the contact region between elastic surface hemispheres and a virtual rigid plane. The parameters of the model are based on estimated values of the asperities (peak heights) and their radius, determined by statistical analysis of measured surface profiles.

In principle, the longitudinal electric breakdown strength of an interface between insulating solids can approximately be expressed by Equation (1). Here, the resulting breakdown strength is considered as the total strength provided by the dimension and number of all series connected interface voids and contact areas. In the case of wet samples, it is reasonable to assume that all interface voids are filled with liquid water, electrically short-circuiting the void. This is a valid assumption at all voltage frequencies below 50 Hz due to the high permittivity ($\varepsilon_r \sim 80$) and high electrical conductivity of tap water ($\sigma \sim 5 \cdot 10^{-3}$ S/m). Thus, at a wet interface, the applied longitudinal voltage (V_{app}) becomes distributed along the interface contact regions only:

$$V_{app} = \cancelto{\approx 0}{\sum_{j=1}^{n} V_{void_j}} + \sum_{k=1}^{m} V_{cnt_k} \approx \sum_{k=1}^{m} V_{cnt_k}\,, \qquad (1)$$

where n and m are the total numbers of cavities and contact spots, respectively, V_{void_j} is the voltage drop across the j^{th} void, and V_{cnt_k} is the voltage drop across the k^{th} contact area located between two voids, as illustrated in Fig. 1.

Since high/local electric field enhancements likely occur at the sharpest tips of the water-filled void enclosures, it is reasonable to assume that the longitudinal electric breakdown strength mainly becomes determined by the resulting field strength and dimensions of the contact areas, as expressed in Equation (1) where V_{cnt_k} is the product of the electric field strength and the length of the contact area parallel to the electric field: $E_{cnt_k} \times l_{cnt_k}$.

According to tribological principles, the resulting contact area, A_{re}, can approximately be expressed by the following relation [16]:

$$A_{re} \approx K \frac{p_a A_a}{E' \sqrt{S}}, \qquad (2)$$

where A_a is the apparent area of contact, given by the dimensions of the test samples, p_a is the applied interface pressure, E' represents the composite elastic modulus, while S is a parameter representing the degree of surface roughness (rougher the surface, higher the S value) and K is a dimensionless constant.

Equation (2) shows that the total area of physical contact between the materials is expected to linearly increase with the contact pressure and be reduced in hard/stiffer materials with high surface roughness.

3. Method

3.1. Samples and experimental setup

The samples examined were rectangular prisms cut from 4 mm sheets of either cross-linked polyethylene (XLPE) cable insulation or poly-methyl methacrylate (PMMA). During testing, two identical samples (4 mm x 55 mm x 30 mm) were placed on top of each other and clamped between two Rogowski-shaped electrodes, as shown in Fig. 2. Thus, allowing longitudinal electric stress to be applied along a 4-mm thick interface between the sample sections. For the testing of the wet-mate samples, sample surfaces were immersed in a container filled with tap water before being mounted between the electrodes, while dry samples were assembled in air.

All breakdown tests were performed to prevent external flashover while keeping the setup immersed in transformer oil. In addition, the unintentional ingress of oil into the interface was prevented by applying the surface pressure prior to filling the test chamber with the oil. Appropriate surface pressures, in the range of 9.68–15.5 kg/cm^2 (9.5 – 15.2 bar), were provided using weights applying a mechanical force perpendicular to the interface between the samples, as illustrated in Fig. 2.

During 50 Hz AC breakdown testing, the voltage was generated using a 100 kV transformer and increased until breakdown at a rate of approximately 1 kV/s. In the case of very low frequency (VLF) breakdown testing, the voltage was slowly ramped up at a rate of 1 kV/s using a 100 kV DC source. This rate of voltage change is comparable to that around zero crossing of a 100 kV magnitude, sinusoidal AC voltage at VLF of approximately 0.002 Hz.

All breakdown measurements were performed at room temperature using newly grinded pairs of identical samples. Five equal tests were performed at each set of test parameters, and the results were statistically evaluated using Gauss distributions.

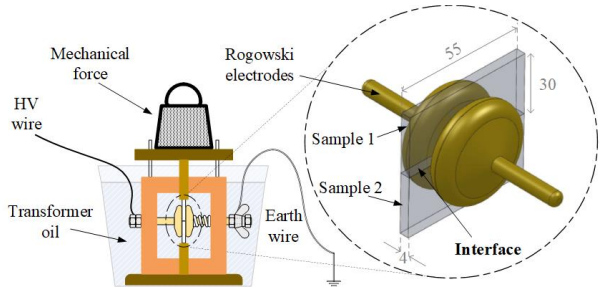

Fig. 2 – Simple illustration of the test setup. The 4 mm-thick solid insulator samples and the electrodes are depicted with their dimensions in mm. Reprinted, with permission, from [12].

3.2. Surface roughness characterization

Prior to assembling, all contact surfaces of the samples were polished using a table-top grinding machine. During this process, the specimens were fixed into a rotating steel frame and were held in contact with a rotating SiC sandpaper of either grit size: 500g or 2000g.

Surface roughness parameters were measured optically using a 3D profilometer (Bruker Contour GT−K). Graphs presented in Figure 3 and the measured values are given in Table 1 clearly demonstrate a high degree of surface roughness in the case of grinding using 500g sandpaper.

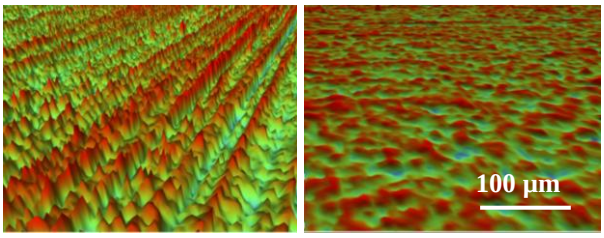

(a) (b)

Fig. 3 – 3D optically measured degrees of surface roughness: (a) Surface of XLPE grinded by sandpaper 500g. (b) Surface of XLPE grinded by sandpaper 2000g.

Modern 3D optical profilometers employ 3D surface texture height parameters (S-parameters) to map the 3D surface textures precisely with reference to ASME Y.14 and ISO 25178–2. Employed S-parameters (height) for this work are namely:

- arithmetic mean height/roughness (S_a),
- RMS height/roughness (S_q),
- the maximum profile peak height (S_p), and
- the minimum profile peak height (S_v).

For instance, the S_a values of each sample in Table 1 can be substituted for the S variable in Equation (1) to obtain an approximate ratio between the real area A_{re} and nominal area A_a. The typical graphs presented in Fig. 3 (and the resulting S-parameters given in Table 1) clearly demonstrate that the highest degree of surface

smoothness is attained in the case of grinding using 2000g sandpaper. Because rougher the surfaces yield larger S, that in turn reduces A_{re}.

Table 1– Measured characteristic values of surface roughness S-parameters of the examined XLPE and PMMA samples.

Sample	Roughness S-parameters [µm]			
	S_a	S_q	S_p	S_v
500g XLPE	0.76	0.97	6.33	-7.89
500g PMMA	0.99	1.27	7.35	-9.10
2000g XLPE	0.44	0.57	3.38	-3.68
2000g PMMA	0.33	0.43	3.72	-3.44

3.3. Elasticity characterization

For comparison, the elasticity of the examined materials was characterized by measuring Young's modulus elasticity using a standard stress-strain test bench with 1 mm thick and 12 mm wide dog-bone-shaped test objects. Typical examples of obtained graphs and measured values are presented in Fig. 4 and Table 2, respectively. The results evidently indicate that PMMA samples are about 3 – 4 times stiffer than XLPE samples. Ideally, microhardness tests are probably more appropriate than the stress-strain tests performed here. The results, however, provide a valuable indication of the relative differences in stiffness between the materials tested.

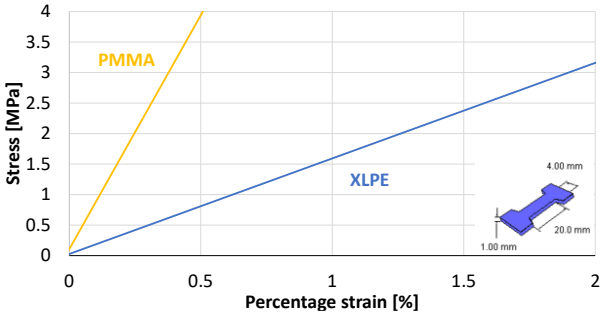

Fig. 4 – Results from stress-strain measurements of Young's modulus of elasticity, using 1-mm thick dog-bone shaped samples of PMMA and XLPE.

Table 2– Measured elastic modulus of each of the examined XLPE and PMMA samples.

Polymer	Poisson's ratio (ν)	Elastic modulus E [MPa]
XLPE	0.46	163
PMMA	0.36	840

The effective elastic modulus of an interface, E', is calculated using the elastic modulus, E, of each material in contact, using the relation below:

$$\frac{1}{E'} = \frac{1}{2}\left(\frac{1-\nu_1^2}{E_1} + \frac{1-\nu_2^2}{E_2}\right), \qquad (3)$$

where E_1, ν_1, and E_2, ν_2 are the elastic modulus and Poisson's ratio of each material in contact, respectively [16]. The calculated effective modulus of each interface formed between identical materials is shown in Table 3.

Table 3– Calculated effective modulus of each interface formed between identical materials using Equation (3).

Interface	Effective-modulus E' [MPa]
XLPE–XLPE	280
PMMA–PMMA	1025

4. Experimental results

Results from initial measurements of longitudinal 50 Hz AC breakdown strength of dry interfaces between XLPE and PMMA samples are shown in Figs. 5 – 6.

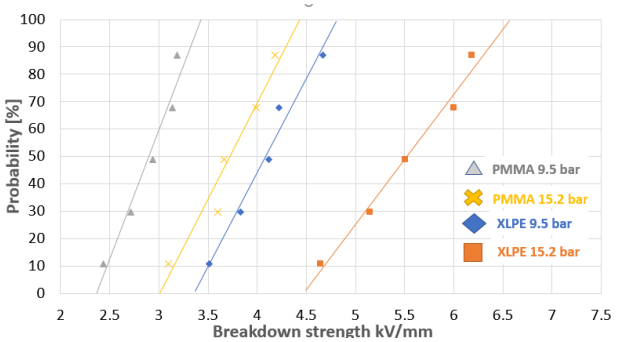

Fig. 5 – The Gauss-probability distribution of measured longitudinal 50 Hz AC breakdown strengths values of interfaces between **dry** XLPE and PMMA samples for the same grit (500g) but varying the interface pressures.

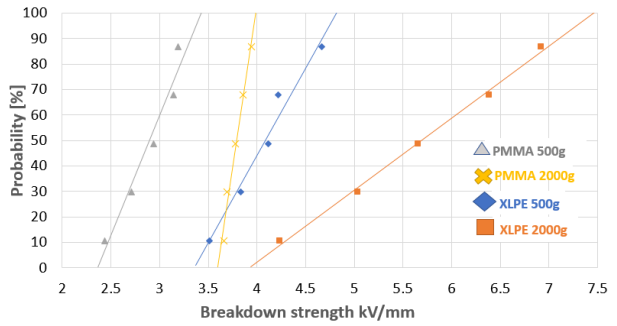

Fig. 6 – Measured longitudinal 50 Hz AC breakdown strength values of interfaces between **dry** XLPE and PMMA samples for the same pressure (9.5 bar) but varying the surface roughness.

The breakdown measurements obtained during AC 50 Hz and VLF breakdown testing of wet samples are presented below in Figs. 7 – 10. The results obtained by AC 50 Hz testing of wet samples are presented in Figs. 7 – 8, whereas those obtained by VLF testing of wet samples are presented below in Figs. 9 – 10. In all examined cases, the VLF breakdown strength was found to be 2 – 3 times higher than at 50 Hz wet samples breakdown tested.

The diagrams shown in Fig. 11 give a more compact summary of some of the measured average breakdown values. It is shown that the breakdown values obtained during VLF breakdown testing typically were 2 – 3 times higher than values obtained in the case of testing at 50 Hz AC voltages. Also, the effect of smoother surfaces in the breakdown strength seems to be much more significant for AC 50 Hz tests than those for VLF.

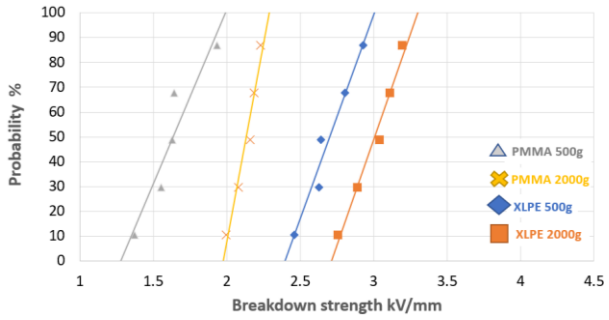

Fig. 7 – Measured longitudinal 50 Hz AC breakdown strength values of interfaces between **wet** XLPE and PMMA samples for the same low pressure (9.5 bar) but varying the surface roughness.

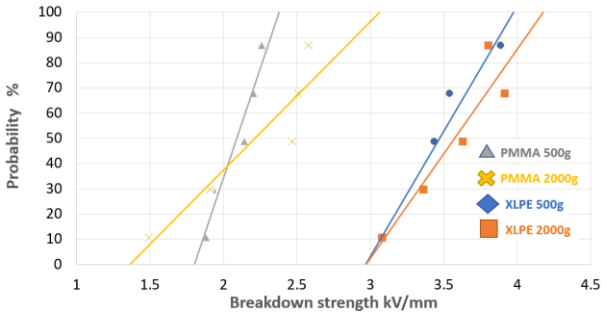

Fig. 8 – Measured longitudinal 50 Hz AC breakdown strength values of interfaces between **wet** XLPE and PMMA samples for the same high pressure (15. 2 bar) but varying the surface roughness.

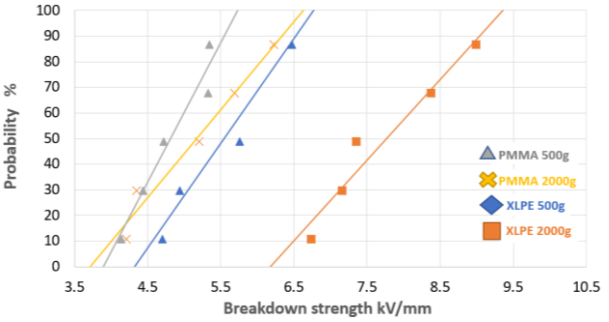

Fig. 9 – Measured values of longitudinal VLF (0.002 Hz) AC breakdown strength of interfaces between **wet** XLPE and PMMA samples at applied low interface pressure (9.5 bar) but varying the surface roughness.

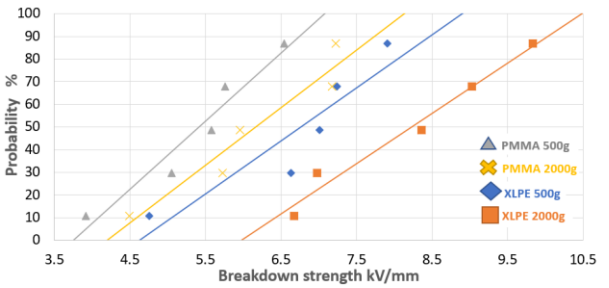

Fig. 10 – Measured values of longitudinal VLF (0.002 Hz) AC breakdown strength of interfaces between **wet** XLPE and PMMA samples at applied high interface pressure (15.2 bar) but varying the surface roughness.

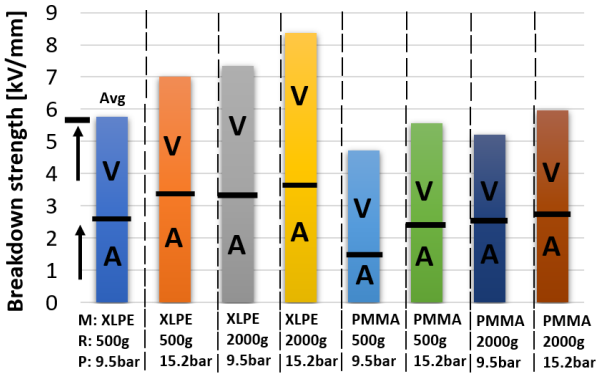

Fig. 11 – Summary of average longitudinal 50 Hz and VLF AC breakdown values, measured using samples of **wet** interfaces. "**A**" indicates the average values for AC 50 Hz wet, and "**V**" indicates the average breakdown strength when VLF is applied to the interfaces regarding the different surface roughness (R), applied mechanical pressures (P), and the differences between the insulation materials that were breakdown tested.

5. Discussion

The resulting longitudinal 50 Hz AC breakdown values of dry XLPE interfaces confirm the previous findings of increased withstand strength and smoother and more compressed interfaces. The breakdown values of wet XLPE samples were found to be approximately 80 % lower than that of comparable types of dry samples. This is an observation in very good agreement with previous findings (see Fig. 8.6 in [17]) and in line with the assumption of higher average longitudinal stress in the case of contact regions connected in series with water-filled surface voids.

In general, wet samples of XLPE showed higher breakdown strength than that made of harder/stiffer PMMA material. In addition, the breakdown strength of XLPE interfaces was found to be most sensitive to variations in surface roughness and interface pressure. This is in accordance with Equation (2), which is based upon tribological principles, that manifests that the average relative dimension of the contact regions is expected to increase inversely proportional to the material hardness (the higher the hardness is, the larger the elastic modulus E' becomes, that in turn reduces A_{re}).

The measured values of elasticity modulus indicate that PMMA is about 3 – 4 times "harder" than XLPE samples taken from cable insulation. The observed AC breakdown strengths of XLPE insulated samples were in all examined cases found to be about 20 – 30 % higher than that of PMMA. Such a discrepancy is likely caused by the fact that the longitudinal electric breakdown strength of an interface depends upon several other unknown factors. The results obtained here, however, indicate a strong correlation between AC breakdown strength and the effective total interface contact area.

The 2 – 3 times higher breakdown strength at VLF voltages compared to that of 50 Hz is likely caused by frequency-dependent electric field distribution and increased probability of rapid ageing at high-frequency testing. At VLF test voltages, partial discharge inception voltage (PDIV) and number of PDs per time unit are likely 100 – 500 times lower than that at 50 Hz, resulting in low tracking rate and electrical tree formation. The

overall effect of this is that during the application of VLF voltages, breakdown occurs at a higher voltage magnitude or after a long time of testing [18]. These observations are also in good agreement with the discussion in [19] that imply that the deposited surface charges have more time to decay further at VLF and thus, do not contribute to the local electric field at polarity reversal as opposed to at 50 Hz; thus increasing the interfacial PDIV and breakdown strength values.

Lastly, elasticity values obtained for the PMMA seem to be significantly smaller than the values stated in the literature. Therefore, the stress-strain measurements addressed in this paper should only be used for comparison, not to be taken as a reference. Other elasticity measurement techniques will be performed to address this discrepancy.

6. Conclusions

Based on the results presented, it can be concluded that:

- The longitudinal AC breakdown strength of wet interfaces strongly increases with increasing dimensions and contact pressure within the distributed regions of surface contacts. The most critical factors are surface roughness, elasticity (hardness), and perpendicularly applied mechanical surface pressure.
- At VLF testing, higher breakdown strength is expected due to the slow rate of electrical tree formation at low voltage frequencies, as the degradation rate is lower than in tests at 50 Hz voltages.

7. References

[1] E. Kantar, D. Panagiotopoulos, and E. Ildstad, 'Factors influencing the tangential AC breakdown strength of solid-solid interfaces', *IEEE Trans. Dielectr. Electr. Insul.*, vol. 23, no. 3, pp. 1778–1788, Jun. 2016, doi: 10.1109/TDEI.2016.005744.

[2] D. Panagiotopoulos, 'AC Electrical Breakdown Strength of Solid Solid Interfaces - A study about the effect of elasticity, pressure and interface conditions', *98*, 2015, Accessed: Nov. 02, 2018. [Online]. Available: https://brage.bibsys.no/xmlui/handle/11250/2368265

[3] M. Hasheminezhad and E. Ildstad, 'Application of contact analysis on evaluation of breakdown strength and PD inception field strength of solid-solid interfaces', *IEEE Trans. Dielectr. Electr. Insul.*, vol. 19, no. 1, pp. 1–7, Feb. 2012, doi: 10.1109/TDEI.2012.6148496.

[4] Y. Luo, Z. Han, M. Zhou, and H. Wang, 'A Sophisticated Method of the Mechanical Design of Cable Accessories Focusing on Interface Contact Pressure', *Energies*, vol. 13, no. 11, Art. no. 11, Jan. 2020, doi: 10.3390/en13112976.

[5] M. Kato, Y. Nishimura, N. Osawa, Y. Yoshioka, H. Yanase, and K. Okamoto, 'Effects of Compressive Force and Dielectric Materials on Contact Area for High-Pressure Region and Interfacial AC Breakdown Between Two Solid Dielectrics', in *Proceedings of the 21st International Symposium on High Voltage Engineering*, Cham, 2020, pp. 118–129. doi: 10.1007/978-3-030-31680-8_13.

[6] A. Ya. Shakhunyants, A. V. Samusenko, and I. F. Safronova, 'The Experimental Setup for Researching Interfacial Breakdown', in *2020 International Youth Conference on Radio Electronics, Electrical and Power Engineering (REEPE)*, Mar. 2020, pp. 1–5. doi: 10.1109/REEPE49198.2020.9059123.

[7] M. Danikas, G. E. Vardakis, and R. Sarathi, 'Some Factors Affecting the Breakdown Strength of Solid Dielectrics: A Short Review', *Eng. Technol. Appl. Sci. Res.*, vol. 10, no. 2, Art. no. 2, Apr. 2020.

[8] M. A. Hamdan, J. A. Pilgrim, and P. L. Lewin, 'Thermo-Mechanical Analysis of Solid Interfaces in HVAC Cable Joints', p. 8.

[9] E. Kantar, 'Dielectric Strength of Polymeric Solid-Solid Interfaces under Dry-Mate and Wet-Mate Conditions', *Energies*, vol. 14, no. 23, Art. no. 23, Jan. 2021, doi: 10.3390/en14238067.

[10] E. Kantar, 'Mechanisms Governing Longitudinal AC Breakdown at Solid-Solid Interfaces', in *2020 IEEE Conference on Electrical Insulation and Dielectric Phenomena (CEIDP)*, Oct. 2020, pp. 279–283. doi: 10.1109/CEIDP49254.2020.9437443.

[11] E. Kantar, F. Mauseth, E. Ildstad, and S. Hvidsten, 'Tangential AC breakdown strength of solid-solid interfaces considering surface roughness', in *2017 IEEE Conference on Electrical Insulation and Dielectric Phenomenon (CEIDP)*, Oct. 2017, pp. 580–583. doi: 10.1109/CEIDP.2017.8257615.

[12] E. Kantar, E. Ildstad, and S. Hvidsten, 'Effect of material elasticity on the longitudinal AC breakdown strength of solid-solid interfaces', *IEEE Trans. Dielectr. Electr. Insul.*, vol. 26, no. 2, pp. 655–663, Apr. 2019, doi: 10.1109/TDEI.2019.008087.

[13] E. Kantar, S. Hvidsten, F. Mauseth, and E. Ildstad, 'A stochastic model for contact surfaces at polymer interfaces subjected to an electrical field', *Tribol. Int.*, vol. 127, pp. 361–371, Nov. 2018, doi: 10.1016/j.triboint.2018.03.003.

[14] E. Kantar, F. Mauseth, E. Ildstad, and S. Hvidsten, 'Longitudinal AC breakdown voltage of XLPE-XLPE interfaces considering surface roughness and pressure', *IEEE Trans. Dielectr. Electr. Insul.*, vol. 24, no. 5, pp. 3047–3054, Oct. 2017, doi: 10.1109/TDEI.2017.006540.

[15] J. A. Greenwood, J. B. P. Williamson, and F. P. Bowden, 'Contact of nominally flat surfaces', *Proc. R. Soc. Lond. Ser. Math. Phys. Sci.*, vol. 295, no. 1442, pp. 300–319, Dec. 1966, doi: 10.1098/rspa.1966.0242.

[16] B. Bhushan, 'Contact mechanics of rough surfaces in tribology: multiple asperity contact', *Tribol. Lett.*, vol. 4, no. 1, pp. 1–35, Jan. 1998, doi: 10.1023/A:1019186601445.

[17] E. Kantar, 'Longitudinal AC Electrical Breakdown Strength of Polymer Interfaces: Experimental and theoretical examination of solid-solid interfaces considering elasticity, surface roughness, and contact pressure', NTNU, 2019. Accessed: Nov. 05, 2019. [Online]. Available: https://ntnuopen.ntnu.no/ntnu-xmlui/handle/11250/2606181

[18] E. Ildstad, 'Electrical properties of insulating materials under VLF voltage', *e-cigre*, vol. WG D1.48, no. ELT_302_6, Jan. 02, 2019. Accessed: Apr. 07, 2022. [Online]. Available: https://e-cigre.org/publication/ELT_302_6-electrical-properties-of-insulating-materials-under-vlf-voltage

[19] E. Kantar, E. Eberg, and S. Hvidsten, 'Effects of Frequency and Temperature on Partial Discharge Characterization of Stator Windings', in *2020 IEEE Conference on Electrical Insulation and Dielectric Phenomena (CEIDP)*, Oct. 2020, pp. 369–373. doi: 10.1109/CEIDP49254.2020.9437438.